Matter of age: growing anisotropic gold nanocrystals in organic media†

Anil V. Gaikwad,[a] Peter Verschuren,[a] Sachin Kinge,[b] Gadi Rothenberg[a] and Erika Eiser‡*[a]

Received 1st October 2007, Accepted 26th November 2007
First published as an Advance Article on the web 17th December 2007
DOI: 10.1039/b715112h

We investigated the influence of the reduction state of gold ions on the growth of gold nanocrystals in *N*,*N*-dimethyl formamide (DMF). While freshly prepared solutions of $AuCl_3$ produce spherical nanocrystals, aged precursor solutions containing mainly Au^+ ions and Au^0 atoms lead to various branched nanoparticles. Furthermore, we show that also the amount of the reducing and stabilisation agent tetra-*n*-octylammonium formate (TOAF) plays a decisive role on the shape of the nanocrystals, allowing us to grow triangular and cubic nanoparticles.

Introduction

Synthesising metal nanoparticles using "bottom-up" techniques is attracting much attention due to their applications in catalysis,[1–4] optoelectronics,[5,6] biological labeling,[7] fuel cells[8] and materials science.[9] Nanometric metal crystals display unique physico-chemical properties that stem from their size and shape. Several studies have achieved excellent control over particle size for both metallic and semiconductor nanocrystals. However, although scientists have managed to make a variety of nanosized crystal shapes including rods,[10–13] triangular prisms,[14–17] disks,[18–20] and even cubes,[21] understanding the factors that govern shape control remain a challenge.[22]

In many applications, crystal anisotropy is a key factor. Nanocrystals with different shapes exhibit different optical and electronic properties, and consequently a variation in the surface-plasmon resonance. To exploit those activities, branched and multipod structures have been made. The most common recipe for making such crystals is the seeded growth of anisotropic particles in water.[23–28] The formation of triangular, hexagonal, decahedral and cubic particles, as well as nanowires, was also reported in DMF and pyridine.[29–32] In all those studies, the interaction of the stabiliser with metal ions and the form of the seeds play a crucial role in controlling the final particles' size and morphology (for example, El-Sayed *et al.* showed that the particles' shape can be controlled by changing the capping ratio of metal ions to stabiliser[33–35]).

Recently, we studied the preparation and catalytic applications of various metal nanoparticles (Pd, Ru, Ni, Ag, and Cu) in DMF and toluene using tetraoctyl ammonium carboxylate salts as reducing and stabilizing agents.[36–38] In all these cases, we obtained spherical particles. Extending this work to gold nanocrystals, we were surprised to find, using the same synthesis method, a variety of nanocrystal shapes. Although different well defined shapes of gold nanocrystals are reported, the formation of branched particles for this particular system in DMF was never reported. We thus began to investigate the cause of these different morphologies. In contrast to aqueous solutions, where a reducing agent is needed for initiating the nanoparticle formation, DMF and formamide can themselves reduce silver and gold salts partially or completely.[39–43] In the present work, we investigate the factors that govern the formation of anisotropic gold particles in DMF using tetraoctylammonium ions as a stabiliser. We show that precursor aging and reducing agent concentration influence the concentration of Au^{3+} and Au^+ ions. This, in turn, affects the rates of Au^0 seed formation and nanoparticle growth.

Experimental

Detailed experimental procedures including description of the materials and instrumentation used in this study are given in the supporting information. Four types of samples (**A**, **B**, **C**, and **D**) were prepared. Sample **A**: 0.5 mM $AuCl_3$ solution in DMF was prepared and aged in a closed vessel under air for 15 to 18 h. Subsequently, 75 μl of 100 mM TOAF in DMF was added to 2 ml of this aged solution. The mixture was then heated to 65 °C and stirred under N_2 for 1 h. Sample **B**: Fresh 0.5 mM $AuCl_3$ solution in DMF was prepared. Immediately after dissolution 60 μl of 100 mM of TOAF/DMF was added to 2 ml of this fresh solution. The sample was then heated to 65 °C and stirred under N_2 for 1 h. Sample **C**: For control experiments 2 ml of fresh 0.5 mM AuCl solution in DMF was prepared that contains only Au^+ ions in contrast to sample **B** containing mainly Au^{3+} ions. As in sample **B**, immediately after dissolution 60 μl of 100 mM TOAF in DMF was added, and the mixture was heated to 65 °C and stirred under N_2 for 1 h. Sample **D**: 2 ml of fresh 0.5 mM $AuCl_3$ solution in DMF was mixed with 50 μl of 200 mM TOAF in DMF then heated and stirred for 1 h under the same conditions as in sample **A** and **B**. This experiment was repeated with 60 and 70 μl of 200 mM TOAF in DMF.

[a] *van 't Hoff Institute for Molecular Sciences, University of Amsterdam, Nieuwe Achtergracht 166, 1018 WV Amsterdam, The Netherlands. E-mail: eiser@science.uva.nl; Fax: +31 20 525 5604*
[b] *MESA+ Institute for Nanotechnology, University of Twente, P.O. 217, 7500 AE Enschede, The Netherlands*

† Electronic supplementary information (ESI) available: Detailed experimental procedures including description of the materials and instrumentation used. See DOI: 10.1039/b715112h

‡ Present address: Cavendish Laboratory, University of Cambridge, J. J. Thomson Avenue, Cambridge, UK CB3 0HE.

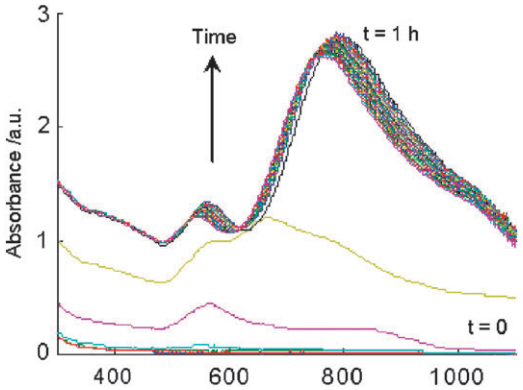

Fig. 1 UV-visible spectra of anisotropic Au-nanoparticle formation in sample **A**. The lowest curve indicates the starting situation, $t = 0$, of the nanoparticle growth.

Results and discussion

We started by synthesizing gold nanoparticles following the method of Reetz and Maase,[44] using $AuCl_3$ in DMF as salt precursor solution and tetra-*n*-octylammonium formate (TOAF) as reducing and stabilising agent. This method was expected to yield spherical nanoparticles with a narrow size distribution. For sample **A** the colourless $AuCl_3$ precursor solution was prepared a day in advance, a fact that at the time seemed unimportant and innocuous. After nanoparticle formation this sample appeared blue and clear in transmission but brown and turbid in reflection (we did not observe any aggregate precipitation). In order to characterise the cluster growth we monitored the evolution of sample **A** *in situ* using UV-visible spectroscopy. At $t = 0$, the moment the reducing agent was added we observed neither the typical absorption peak of the Au^{3+} ion precursor ($\lambda = 322$ nm) nor the surface-plasmon peak typical for Au spherical nanocrystals ($\lambda \sim 550$ nm). Instead, we observed the evolution of a surface plasmon peak at *ca.* 790 nm with a shoulder at 590 nm (Fig. 1), typical of samples containing anisotropic nanoparticles.[45,46] The reaction was completed after 1 h rendering sample **A** stable for over four weeks at 25 °C. Further characterisation of sample **A** by HRTEM showed indeed variously shaped particles, roughly 40–80 nm in diameter (Fig. 2). A close up view showed different particle shapes including bipods, tripods, tetrapods, and branched nanoparticles.

To investigate this phenomenon further we prepared gold nanoparticles from a freshly prepared $AuCl_3$ precursor solution (sample **B**). Here, TOAF was immediately added to the fresh solution and kept at 65 °C for 1 h, like in sample **A**. Monitoring this reaction using UV-visible spectroscopy, initially ($t = 0$) we observed only the absorption peak of the free Au^{3+} ions (Fig. 3). However, within a few minutes this Au^{3+} peak decreased to zero, followed by a clear surface plasmon peak emerging at ~600 nm. A TEM analysis confirmed that sample **B** contains mainly spherical particles, with a narrow size distribution of 14 ± 2.0 nm. To ensure reproducibility, triplicate experiments were carried out in each case. In all cases, freshly prepared solutions of $AuCl_3$ in DMF led to the formation of spherical gold nanocrystals with an average diameter of ~15 nm. For control we also repeated the reduction experiments with aged (colourless) precursor samples following the preparation protocol for sample **A**. Once again we obtained anisotropic gold nanoparticles with similar shapes and size (see ESI, Fig. S2)† as those shown in Fig. 2.

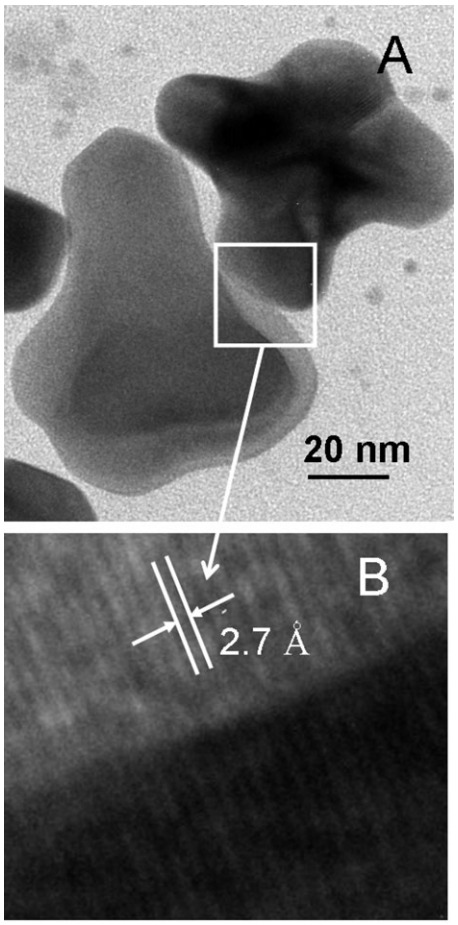

Fig. 2 (A) HRTEM image of branched gold nanocrystals (sample **A**). (B) Blow up of the white square in image (A). The two parallel lines indicate the packing distance between two hexagonally packed dense Au-planes.

To understand this, we first investigated the aging behaviour of $AuCl_3$ in DMF prior to the addition of any reducing agent. Fig. 4 shows the UV-visible absorption spectra of $AuCl_3$ (0.5 mM) in DMF at 25 °C over 20 h under an inert atmosphere. Although no external reducing agent was present, we observed a clear disappearance of the Au^{3+} ion peak at 322 nm. It was reported that DMF reduces Au^{3+} ions under reflux conditions in the presence of a stabilising agent such as (poly)vinylpyrrolidone, giving spherical gold nanoparticles,[43] so we presumed that some reduction could also occur at room temperature. This reaction, however, also requires at least one equivalent of water (eqns (1) and (2)).[47] Karl-Fischer titrations confirmed that the DMF we used contained 0.04% water, or 44 equivalents, sufficient for reducing the Au^{3+} ions to Au^{+} ions and Au^0 atoms. Moreover, while the fresh $AuCl_3$ solution in DMF was neutral, the aged precursor solution was acidic (pH = 4.5), supporting the formation of carbamic acid and H^+ ions *via* eqns (1) or (2).

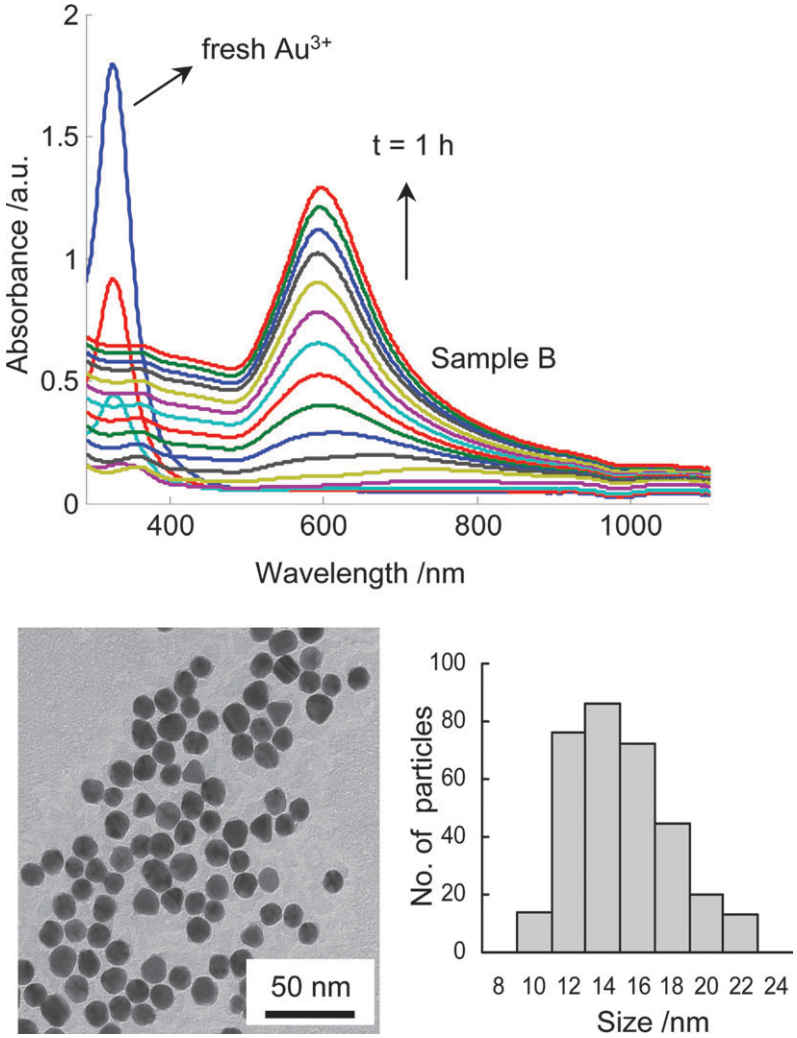

Fig. 3 (Top) Time-resolved *in situ* UV-visible spectra of precursor reduction and nanoparticles formation using the freshly prepared $AuCl_3$ precursor solution **B**. (Bottom left) TEM micrograph of the resulting spherical gold nanoparticles; (bottom right) corresponding size distribution, based on 300 particles counted.

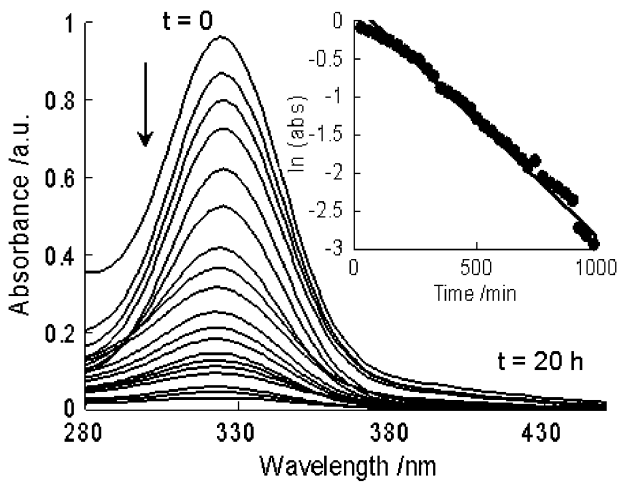

Fig. 4 Time-resolved UV-visible spectra of the reduction of Au^{3+} ions in DMF at 25 °C. The inset shows the rate of reduction in terms of decrease in absorbance of Au^{3+} at λ_{max} = 322 nm *versus* time.

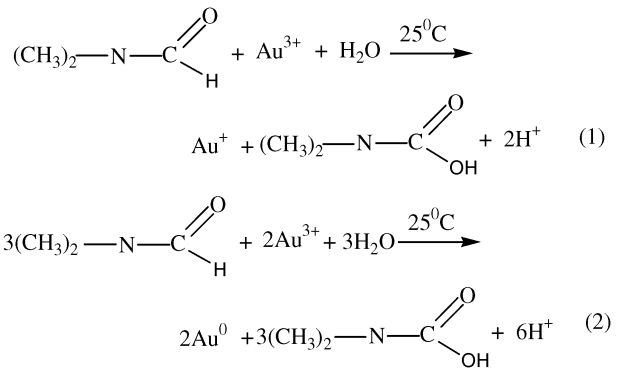

Whether Au^{3+} partially reduces to Au^{+} or completely to Au^{0} in DMF is unknown. Pradeep and co-workers hypothesised that Au^{3+} reduces completely to Au^{0}, in a similar fashion to Ag, thereby producing carbamic acid.[48] Carbamic acid is unstable in DMF and readily decomposes to $(CH_3)_2NH$ and CO_2. Similar to Tom *et al.*[48] we performed infrared

spectroscopy (IR) and gas chromatography-mass spectroscopy (GC-MS). However, their weak signal was dominated by the strong contributions from DMF. We surmised that our aged $AuCl_3$ precursor solution contained both Au^+ and Au^0 species. This was confirmed by cyclic voltammetry studies of aged and fresh gold precursor solutions. While the fresh solution showed two reduction peaks for $Au^{3+} \rightarrow Au^+$ (E_v = 0.49 V) and $Au^+ \rightarrow Au^0$ (E_v = 0.95 V), respectively, the aged solution showed only one, corresponding to $Au^+ \rightarrow Au^0$ (E_v = 1.05 V; the cyclic voltammograms are included in the supporting information, Fig. S1). Freshly dissolved AuCl–DMF solutions also showed only one reduction peak, agreeing well with our observations in aged solutions. Based on these findings we hypothesise that next to Au^+ ions the presence of Au^0 atoms or neutral gold seed of less than 1 nm in size is necessary to initiate the formation of gold nanocrystals in DMF.

To test our hypothesis we then prepared sample **C**, starting from fresh AuCl precursor solutions in DMF containing only Au^+ ions similar to the aged solution, and using the same amount of the reducing and stabilising agent TOAF as in sample **B**. As expected we did not observe any nanoparticle formation. The reduction potential of Au^+ ions to Au^0 atoms is higher than that of Au^{3+} ions.[38] This showed that the aged solution contained both Au^+ ions and Au^0 that can form a complex with DMF. Gold nanoparticles have a high electron affinity and can strip off electrons from the DMF molecules.[49] The resulting complexes act as seeds for further reduction of Au^+ ions (the so-called aurophilic effect[50]), and grow to give branched particles when the reducing agent TOAF was added, as demonstrated in Fig. 1. Such particle growth in liquid media involves mainly two factors: one is the influence of the capping agent, that controls the growth on the various crystal facets.[51] The second is the rate of supply of Au^0 to the crystal planes of the growing seed particles. A third influence can arise due to surface autocatalytic reduction of Au^+ ions at the gold nanocrystals surface, but may not be as effective as the first two, as it is limited to a rather small available surface area.[52–55] Thus, the shape and size of the seed play an important role.[56] To understand the effect of the second factor we compared the rate of increase in intensity of the surface plasmon peaks in samples **A** and **B** (Fig. 5).

Comparing the aged precursor (sample **A**) to the fresh precursor (sample **B**), we see that in **A** the surface plasmon appears fast and the absorption increases, reaching a plateau after ~5 min. Conversely, **B** exhibits a prolonged reduction period reaching a plateau only after 25 min. Sample **A** shows almost no induction period. This probably reflects the fact that some of the Au^{3+} ions are already reduced to Au^0 atoms or Au^{1+} ions in DMF, and subsequently form sub-nanometer seed particles that are too small to show a plasmon peak.[57] When the external reducing agent is added (at t = 0), further reduction of the remaining Au^+ ions and subsequent particle growth are fast, and the different reduction rates at the various crystal surfaces ultimately yield different crystal shapes (*vide infra*). Conversely, in case **B**, the nanoparticles grow uniformly in all directions and the increase of the surface plasmon resonance shows a typical S-shaped curve. This type of curve agrees well with the results of Gan *et al.*[41] The induction

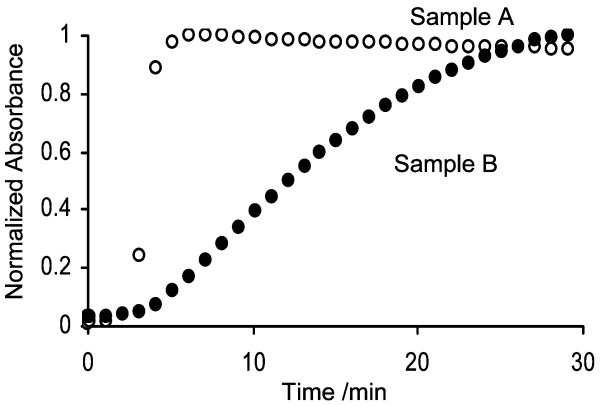

Fig. 5 Change in the normalised surface-plasmon absorption of samples **A** (500–650 nm) and **B** (500–700 nm) *versus* time. In each case the range of wavelengths was used to compensate for the peak shift with particle growth.

period denotes the time to reduce Au^{3+} to Au^0 atoms that nucleate and form sub-nanometric seed particles.[41,58]

To study this effect of rate generation of Au^0 atoms on the nanoparticles morphology, we reduced a fresh Au^{3+} solution using higher TOAF concentrations than in sample **B** (sample **D**). Here we obtained high yields of cubes (60%), prisms (30%), and spherical particles (10%) of 20–30 nm in size (Fig. 6). Importantly, we did not observe any branched particles. We conclude that the shape of the gold nanoparticles depends on the reducing agent concentration as well as on the interaction of the stabiliser with the different crystal surfaces.[59] In fact, a higher ratio of reducing agent to Au^{3+} ions causes monomer super-saturation. This leads to a simultaneous nucleation and growth process resulting in anisotropic particles, especially with "soft metals" like gold. Conversely, hard metal nanocrystals such as Pd, Pt and Cu yield mainly spherical nanoparticles, their size depending only on the concentration of TOAF as reducing and stabilising agent.[58]

The formation of multipod shapes is associated with the rate of supply of Au^0 atoms to (1,1,1), (1,1,0) and (1,0,0) crystal planes.[24,60] The corresponding surface energy[61] increases in the order $Au_{(1,1,1)} < Au_{(1,0,0)} < Au_{(1,1,0)}$. The tetraoctylammonium species adsorb preferentially on the low-energy (1,1,1) surface, leaving the other surfaces open for further crystal growth. The formation of spherical, cubic, prism, or branched shapes depends on the local concentration of Au^0 atoms. In the case of sample **B**, where the formation of Au^0 atoms is slow and hence the local concentration is low, the rate of association/dissociation of the tetraoctylammonium species is similar to that of the Au^0 atoms, resulting in spherical particles. Conversely, sample **D** has a high concentration of Au^0, which causes an imbalance that promotes growth on the available (1,1,0) and (1,0,0) planes, resulting in cubes and prisms, respectively. In case of sample **A**, the crystals grow simultaneously on the (1,0,0) and the (1,1,0) planes, resulting in multipod structures.[25] Finally, we note that the preferential adsorption of halide counterions onto the different crystallographic surfaces of the gold particles may have an influence on the shape morphism.[62,63] In the present study this influence can be neglected as we only considered Cl^- counterions.

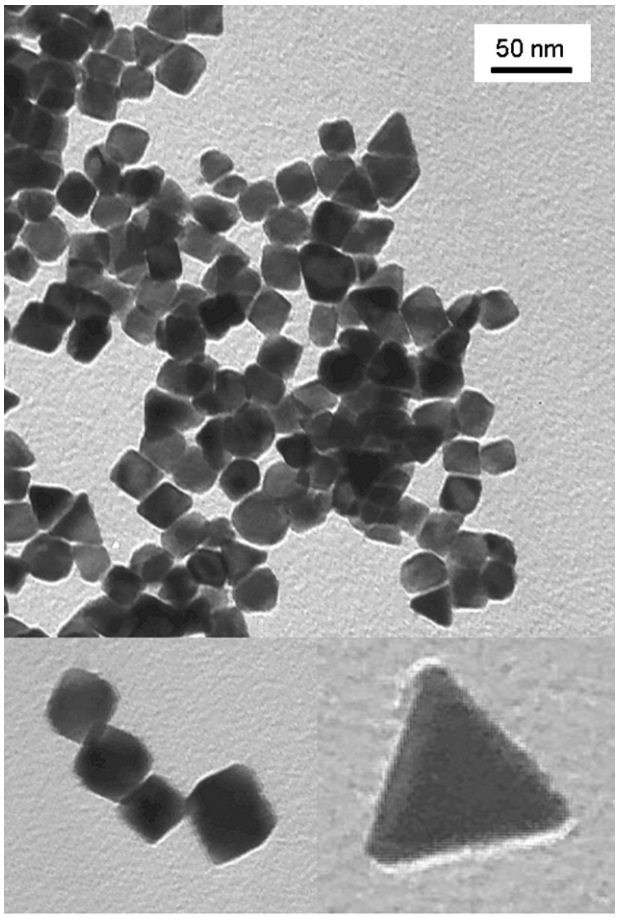

Fig. 6 TEM images of nanoprisms and nanocubes prepared using fresh $AuCl_3$ precursor solution with higher TOAF concentration (sample **D**, 60% cubic, 30% triangular and 10% spherical particles, based on 100 particles counted).

Conclusion

The shape and size of gold nanoparticles depend strongly on the concentration of the reducing agent and the presence of sub-nanometric seed particles. While using DMF as a solvent one should take into account that the solvent DMF can already reduce Au^{3+} ions to Au^{+}/Au^{0} (even though this process is much slower than the reduction in the presence of TOAF). The reduction processes of Au^{+} and Au^{3+} are distinct, and can be followed using cyclic voltammetry. Changing the concentration of the reducing agent and controlling the freshness of the precursor solution, gives access to isotropic or anisotropic gold nanoparticles (including cubes, prisms, and branched particles).

Acknowledgements

We thank T. Franssen-Verheijen (Wageningen University) for performing the TEM analysis, J. H. Blank for the Karl-Fischer measurements, C. Mahabiersing and Dr F. Hartl for the cyclic voltammetry measurements and Dr M. C. Mittelmeijer-Hazeleger (all from the University of Amsterdam) for technical assistance. This research was funded by the Netherlands Organization for Scientific Research (NWO) Vernieuwingsimpuls program.

References

1 A. Roucoux, J. Schulz and H. Patin, *Chem. Rev.*, 2002, **102**, 3757.
2 H. Bönnemann and R. M. Richards, *Eur. J. Inorg. Chem.*, 2001, 2455.
3 C. R. LeBlond, A. T. Andrews, Y. Sun and J. R. Sowa, Jr, *Org. Lett.*, 2001, **3**, 1555.
4 B. D. Chandler and L. H. Pignolet, *Catal. Today*, 2001, **65**, 39.
5 P. V. Kamat, *J. Phys. Chem. B*, 2002, **106**, 7729.
6 C. J. Murphy, T. K. Sau, A. M. Gole, C. J. Orendorff, J. Gao, L. Gou, S. E. Hunyadi and T. Li, *J. Phys. Chem. B*, 2005, **109**, 13857.
7 S. R. Nicewarner-Pena, R. Griffith Freeman, B. D. Reiss, L. He, D. J. Pena, I. D. Walton, R. Cromer, C. D. Keating and M. J. Natan, *Science*, 2001, **294**, 137.
8 S. S. C. Chuang, *Catalysis*, 2005, **18**, 186.
9 S. Nie and S. R. Emory, *Science*, 1997, **275**, 1102.
10 S. Link and M. A. El-Sayed, *J. Phys. Chem. B*, 1999, **103**, 8410.
11 Y.-Y. Yu, S.-S. Chang, C.-L. Lee and C. R. C. Wang, *J. Phys. Chem. B*, 1997, **101**, 6661.
12 X. Peng, U. Manna, W. Yang, J. Wickham, E. Scher, A. Kadavanich and A. P. Allvisatos, *Nature*, 2000, **404**, 59.
13 N. R. Jana, L. Gearheart and C. J. Murphy, *J. Phys. Chem. B*, 2001, **105**, 4065.
14 R. Jin, Y. Cao, C. A. Mirkin, K. L. Kelly, G. C. Schatz and J. G. Zheng, *Science*, 2001, **294**, 1901.
15 Y. Sun, B. Mayers and Y. Xia, *Nano Lett.*, 2003, **3**, 675.
16 S. Chen and D. L. Carroll, *Nano Lett.*, 2002, **2**, 1003.
17 G. S. Metraux, Y. C. Cao, R. Jin and C. A. Mirkin, *Nano Lett.*, 2003, **3**, 519.
18 M. Maillard, S. Giorgio and M.-P. Pileni, *Adv. Mater.*, 2002, **14**, 1084.
19 V. F. Puntes, D. Zanchet, C. K. Erdonmez and A. P. Alivisatos, *J. Am. Chem. Soc.*, 2002, **124**, 12874.
20 M. Maillard, P. Huang and L. Brus, *Nano Lett.*, 2003, **3**, 1611.
21 Y. G. Sun and Y. N. Xia, *Science*, 2002, **298**, 2176.
22 C. J. Murphy, *Science*, 2002, **298**, 2139.
23 E. Hao, R. C. Bailey, G. C. Schatz, J. T. Hupp and S. Li, *Nano Lett.*, 2004, **4**, 327.
24 T. K. Sau and C. J. Murphy, *J. Am. Chem. Soc.*, 2004, **126**, 8648.
25 S. H. Chen, Z. L. Wang, J. Ballato, S. H. Foulger and D. L. Carroll, *J. Am. Chem. Soc.*, 2003, **125**, 16186.
26 C.-H. Kuo and M. H. Huang, *Langmuir*, 2005, **21**, 2012.
27 C. L. Nehl, H. Liao and J. H. Hafner, *Nano Lett.*, 2006, **6**, 683.
28 M. Yamamoto, Y. Kashiwagi, T. Sakata, H. Mori and M. Nakamoto, *Chem. Mater.*, 2005, **17**, 5391.
29 T. C. Deivaraj, N. L. Lala and J. Y. Lee, *J. Colloid Interface Sci.*, 2005, **289**, 402.
30 Y. Chen, X. Gu, C.-G. Nie, Z.-Y. Jiang, Z.-X. Xie and C.-J. Lin, *Chem. Commun.*, 2005, 4181.
31 M. Giersig, I. Pastoriza-Santos and L. M. Liz-Marzán, *J. Mater. Chem.*, 2004, **14**, 607.
32 A. Sanchez-Iglesias, I. Pastoriza-Santos, J. Perez-Juste, B. Rodriguez-Gonzalez, F. J. G. de Abajo and L. M. Liz-Marzan, *Adv. Mater.*, 2006, **18**, 2529.
33 T. S. Ahmadi, Z. L. Wang, T. C. Green, A. Henglein and M. A. ElSayed, *Science*, 1996, **272**, 1924.
34 B. Nikoobakht and M. A. El-Sayed, *Chem. Mater.*, 2003, **15**, 1957.
35 S. Eustis and M. A. El-Sayed, *Chem. Soc. Rev.*, 2006, **35**, 209.
36 L. Durán Pachón, J. H. van Maarseveen and G. Rothenberg, *Adv. Synth. Catal.*, 2005, **347**, 811.
37 M. B. Thathagar, J. Beckers and G. Rothenberg, *J. Am. Chem. Soc.*, 2002, **124**, 11858.
38 J. Wang, H. F. M. Boelens, M. B. Thathagar and G. Rothenberg, *ChemPhysChem*, 2004, **5**, 93.
39 I. Pastoriza-Santos and L. M. Liz-Marzan, *Pure Appl. Chem.*, 2000, **72**, 83.
40 A. Sarkar, S. Kapoor and T. Mukherjee, *J. Phys. Chem. B*, 2005, **109**, 7698.
41 M. Y. Han, C. H. Quek, W. Huang, C. H. Chew and L. M. Gan, *Chem. Mater.*, 1999, **11**, 1144.

42 I. Pastoriza-Santos and L. M. Liz-Marzan, *Langmuir*, 1999, **15**, 948.
43 I. Pastoriza-Santos and L. M. Liz-Marzan, *Langmuir*, 2002, **18**, 2888.
44 M. T. Reetz and M. Maase, *Adv. Mater.*, 1999, **11**, 773.
45 S. Underwood and P. Mulvaney, *Langmuir*, 1994, **10**, 3427.
46 C. S. Weisbecker, M. V. Merritt and G. M. Whitesides, *Langmuir*, 1996, **12**, 3763.
47 Y. J. Yu, S. Schreiner and L. Vaska, *Inorg. Chim. Acta*, 1990, **170**, 145.
48 R. T. Tom, A. S. Nair, N. Singh, M. Aslam, C. L. Nagendra, R. Philip, K. Vijayamohanan and T. Pradeep, *Langmuir*, 2003, **19**, 3439.
49 K. G. Thomas, J. Zajicek and P. V. Kamat, *Langmuir*, 2002, **18**, 3722.
50 G. Li, M. Lauer, A. Schulz, C. Boettcher, F. Li and J.-H. Fuhrhop, *Langmuir*, 2003, **19**, 6483.
51 C. Lofton and W. Sigmund, *Adv. Funct. Mater.*, 2005, **15**, 1197.
52 C. Besson, E. E. Finney and R. G. Finke, *J. Am. Chem. Soc.*, 2005, **127**, 8179.
53 C. Besson, E. E. Finney and R. G. Finke, *Chem. Mater.*, 2005, **17**, 4925.
54 M. A. Watzky and R. G. Finke, *Chem. Mater.*, 1997, **9**, 3083.
55 M. A. Watzky and R. G. Finke, *J. Am. Chem. Soc.*, 1997, **119**, 10382.
56 H. W. Liao and J. H. Hafner, *J. Phys. Chem. B*, 2004, **108**, 19276.
57 D. G. Duff, A. Baiker and P. P. Edwards, *Langmuir*, 1993, **9**, 2301.
58 A. V. Gaikwad and G. Rothenberg, *Phys. Chem. Chem. Phys.*, 2006, **8**, 3669.
59 A. E. Saunders, M. B. Sigman, Jr and B. A. Korgel, *J. Phys. Chem. B*, 2004, **108**, 193.
60 J. M. Petroski, Z. L. Wang, T. C. Green and M. A. El-Sayed, *J. Phys. Chem. B*, 1998, **102**, 3316.
61 Q. Jiang, H. M. Lu and M. Zhao, *J. Phys.: Condens. Matter*, 2004, **16**, 521.
62 T. H. Ha, H.-J. Koo and B. H. Chung, *J. Phys. Chem. C*, 2007, **111**, 1123.
63 O. M. Magnussen, *Chem. Rev.*, 2002, **102**, 679.

